This study develops a global, multi-year inversion of biogenic isoprene emissions by assimilating CrIS-retrieved isoprene columns into the LMDZ-INCA chemistry—transport model, producing monthly emission estimates for 2013–2020. The approach represents a meaningful advancement in directly constraining isoprene emissions, distinct from traditional HCHO-based inversions. The manuscript is clearly structured, and the results are generally consistent with existing inventories, providing valuable insights into the spatial and interannual variability of global biogenic sources. Overall, I find the study scientifically relevant and well executed, but several methodological and interpretative aspects require clarification before publication.

Response:

We greatly appreciate the referee's valuable and perceptive feedback on our manuscript. Below, we provide detailed responses addressing each point raised.

Model description and chemical mechanism

A more detailed description of the atmospheric transport model (LMDZ-INCA) is needed, particularly the configuration of isoprene-related chemistry and its coupling with oxidants such as OH and NOx. Since the chemical mechanism largely governs how simulated isoprene columns respond to emission perturbations, the manuscript should specify the chemical mechanism (i.e., relevant reaction pathways and key rate constants). This will allow readers to assess the reliability and representativeness of the inversion results.

Response:

We have expanded the description of the VOC chemical mechanisms in the manuscript (Lines 153–160), with particular attention to isoprene and HCHO. Briefly, the LMDZ-INCA model features a comprehensive reactive VOC chemistry scheme that incorporates 14 reactions for isoprene and 80 for HCHO, based on the up-to-date reaction rates.

Lines 153-160 in Section 2.2:

"LMDZ-INCA contains a state-of-the-art CH₄–NO_x–CO–NMHC–O₃ tropospheric photochemistry scheme with a total of 174 tracers, including the chemical degradation scheme of 10 non-methane hydrocarbons (NMHCs): C₂H₆, C₃H₈, C₂H₄, C₃H₆, C₂H₂, a lumped C>4 alkane, a lumped C>4 alkene, a lumped aromatic, isoprene and α-pinene. The mechanism comprises 398 homogeneous, 84 photolytic, and 33 heterogeneous reactions, and is continuously updated to integrate newly identified chemical processes and reaction pathways, thereby improving the representation of atmospheric composition and oxidation capacity (Hauglustaine et al., 2004; Folberth et al., 2006; Pletzer et al., 2022; Sand et al., 2023; Terrenoire et al., 2022; Novelli et al., 2020; Wennberg et al., 2018). Reactions directly related to isoprene and HCHO are listed in Tables S1-S2."

Sensitivity to NOx levels

Given that the oxidation rate of isoprene depends on ambient NOx conditions, it would be valuable to perform an additional sensitivity experiment under NO2 concentrations closer to TROPOMI observations.

Response:

We performed a sensitivity experiment by increasing NO_x emission inputs by 25% for the year 2019. This adjustment resulted in a closer agreement of simulated NO_2 from LMDZ-INCA with TROPOMI observations, alleviating the original underestimation (Fig. S13). The global annual total from this inversion differs by less than 1% from the base inversion, with the largest regional deviation found in South Asia (SAS). The results of this sensitivity test have been added in Lines 270–273 in the manuscript and illustrated in Fig. S14.

Lines 270–273:

"To further assess the influence of NO_x conditions on the inversion, we perform a sensitivity test using +25% NO_x emissions for 2019. The results show negligible differences from the base inversion, with a global annual total deviation of less than 0.1% and the largest regional difference of 0.9% over South Asia (SAS) (Fig. S14)."

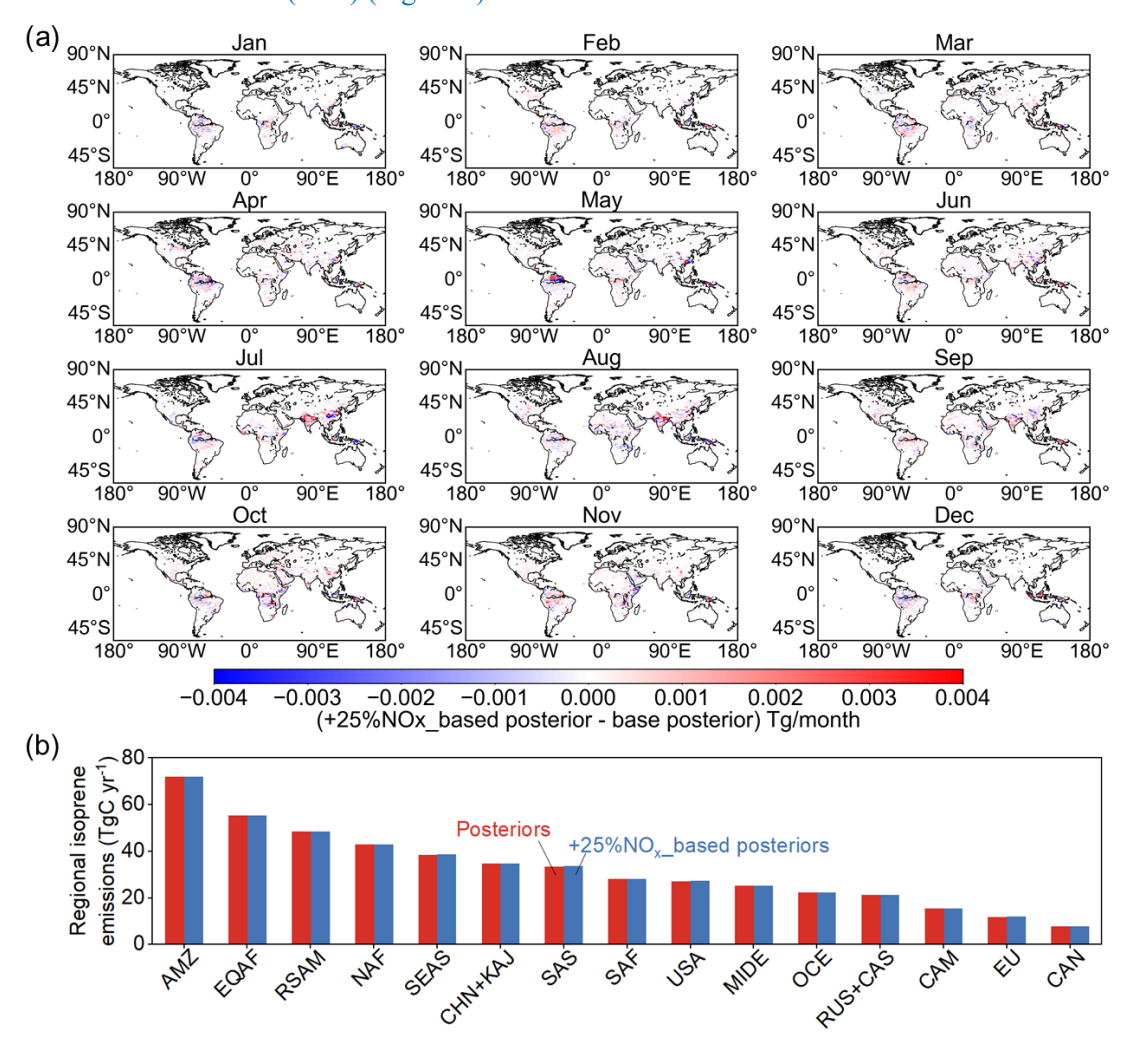


Figure S14. Comparison between base inversion and sensitivity inversion with $\pm 25\%$ NO_x emission input. (a) presents the global distribution of monthly difference in isoprene posteriors, and (b) compares the regional annual isoprene posteriors.

Seasonality of posterior emissions

The seasonality of posterior emissions in this study appears to differ from that of existing inventories, yet the underlying cause of this discrepancy remains unclear. It would be helpful to disentangle the contributions from the prior and the observational constraint. I suggest presenting the seasonal cycles of the prior (e.g., ORCHIDEE), satellite observations (CrIS isoprene and satellite HCHO), and possibly a parallel inversion using MEGAN as the prior. Comparing these seasonal patterns would clarify whether the retrieved seasonality reflects model, data adjustments, or inherent observational features, thereby strengthening the validation of the inferred isoprene emission seasonality.

Response:

To evaluate the robustness of the seasonal pattern identified in this study, we conducted sensitivity inversions for 2019 using MEGAN-MACC and MEGAN-ERA5 as alternative isoprene priors. Both inversions produce posterior emissions that peak during JAS and reach a minimum in DJF, consistent with our posteriors. In addition, satellite-observed isoprene and HCHO column concentrations display similar seasonal variations, supporting the reliability of the posterior peak in JAS and minimum in DJF. These consistent seasonal features across the HCHO-based isoprene inversion, prior sensitivity tests, and satellite observations have been incorporated in Lines 363–366, 374–378, Figure 3, and Figure S20.

Lines 363-366:

"This seasonal cycle agrees with recent HCHO-based inversion results (Müller et al., 2024) but differs markedly from that in current bottom-up inventories: MEGAN-MACC (Sindelarova et al., 2014) and MEGAN-ERA5 (also known as CAMS-GLOB-BIOv3.1) (Sindelarova, 2021; Sindelarova et al., 2022) (Figs. 3 and S20)."

Lines 374-378:

"Besides, sensitivity inversions using MEGAN-MACC and MEGAN-ERA5 as priors also reproduce a JAS maximum and DJF minimum, reversing the original prior seasonality. The posterior seasonality derived from all three priors aligns with that observed in CrIS isoprene and OMPS HCHO concentrations (Fig. S20), indicating that the retrieved temporal variability reflects the observed atmospheric signals and demonstrating the robustness of the inferred seasonal cycle."

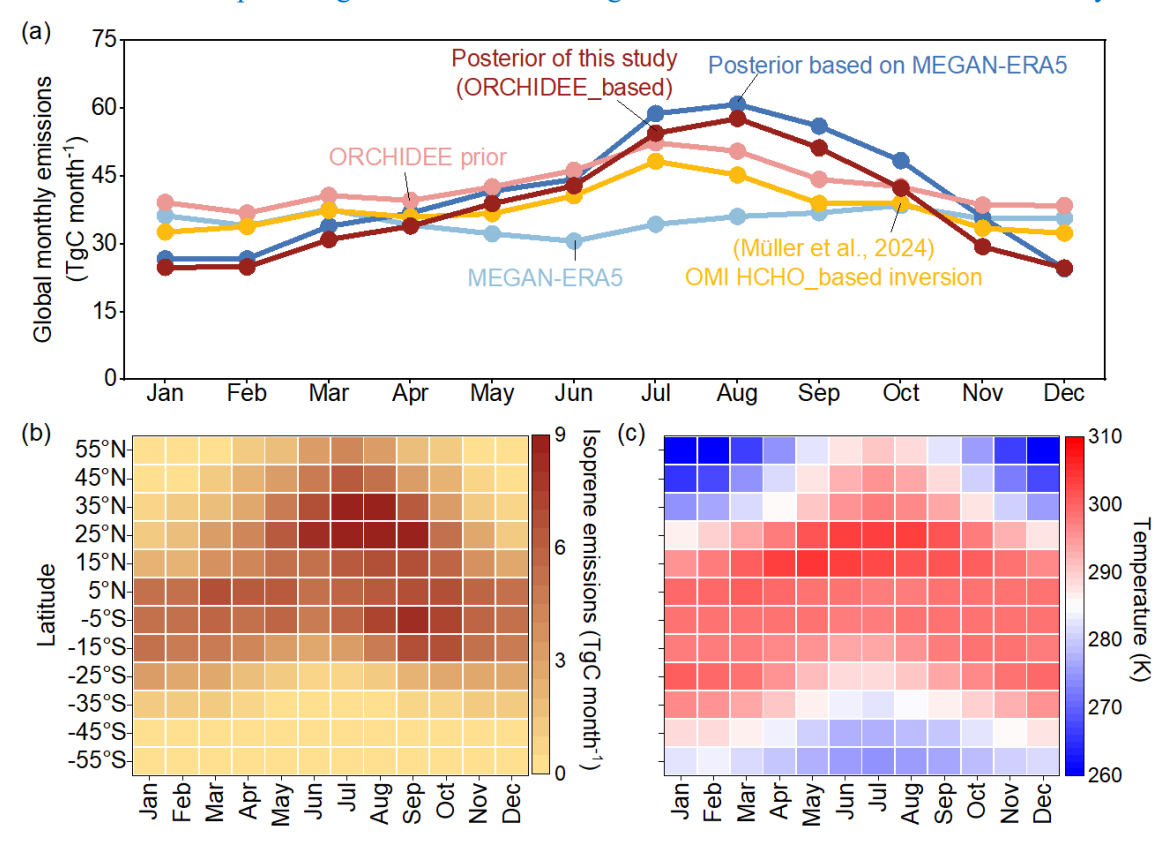


Figure 3. Monthly mean isoprene emissions from 2013 to 2020. (a) shows the global monthly pattern of ORCHIDEE prior and our posterior in this study, MEGAN-ERA5 (also known as CAMS-GLOB-BIOv3.1) inventory (Sindelarova, 2021) and posterior based on MEGAN-ERA5, as well as OMI HCHO-based isoprene inversion result (Müller et al., 2024). MEGAN-ERA5 is based on MEGAN v2.1, updated with ERA5 meteorology and CLM4 land cover (Sindelarova et al., 2022).

(b)-(c) display monthly distributions of our estimated isoprene emissions (TgC) and temperature (K) by every 10° latitude band, respectively. We here only present the latitude range from 60°S to 60°N where emissions dominate (~99%). Temperature is acquired from ERA5. The monthly distributions of two MEGAN inventories (MEGAN-MACC and MEGAN-ERA5), precipitation from ERA5, and the Leaf area index (LAI) from Pu et al. (2024) are presented in Fig. S25.

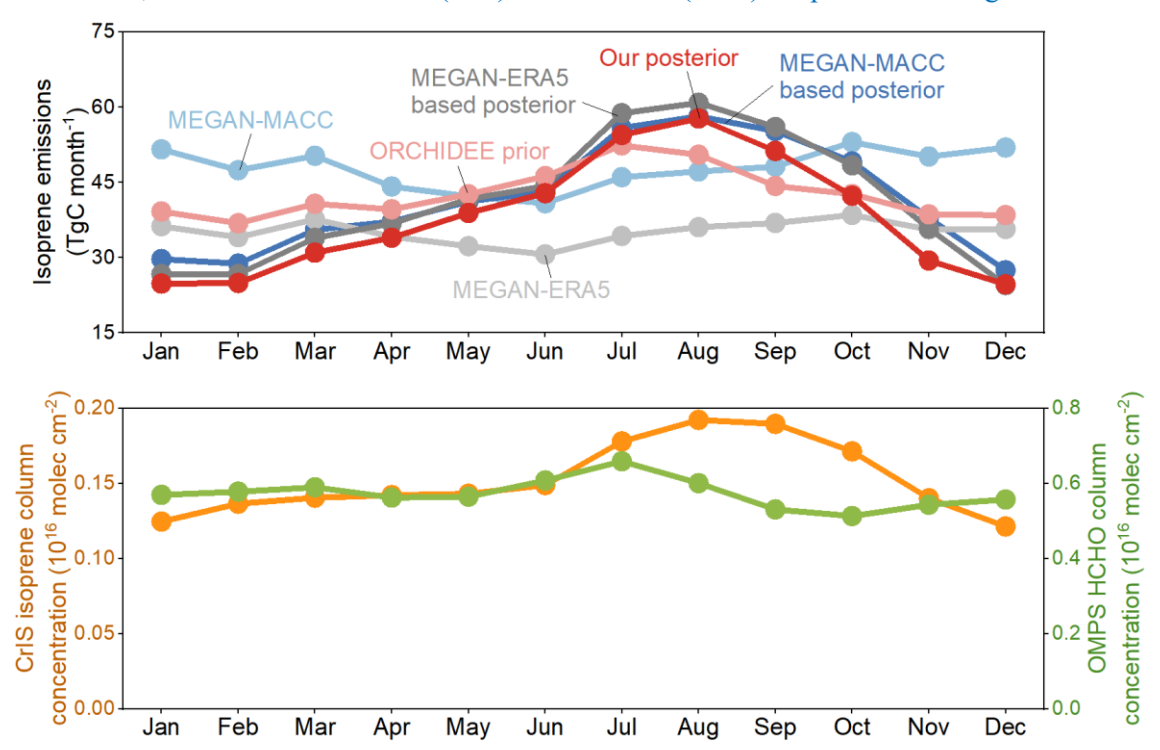


Figure S20. Monthly variation of isoprene emissions (ORCHIDEE prior and posterior, MEGAN-MACC prior and posterior, MEGAN-ERA5 and posterior) and CrIS observed isoprene column and OMPS HCHO column concentrations.

Regional contribution and structure of Sections 3.5–3.6

Section 3.5 could be more focused on quantifying and interpreting regional contributions to global variability, while Section 3.6 emphasizes the environmental drivers. This clearer separation would improve the logical flow and avoid redundancy between the two sections. Additionally, including comparisons with MEGAN or other inventories in the driver analysis (Section 3.6) would contextualize the inversion results and highlight the added value of the CrIS-based framework in capturing regional differences and environmental controls on isoprene emissions.

Response:

We have streamlined Sections 3.5 and 3.6 to make the discussion more concise and focused. Section 3.5 now highlights the regional contributions to global inter-phase variations, whereas Section 3.6 concentrates on the analysis of key environmental drivers and includes comparisons with the MEGAN-ERA5 inventory. Please refer to Section 3.5 and 3.6 for details.

Specific comments:

Line 125: Please specify the TROPOMI NO2 version.

Response:

The TROPOMI NO₂ we adopted is TROPOMI-RPRO-v2.4. We have added this information in Line 126.

Section 3.2: In the current uncertainty configuration, the authors apply a simplified three-segment scheme for the CrIS observational uncertainty, assigning a uniform 70% uncertainty for all low-column grids. This assumption may underestimate the uncertainty gradient in regions with very low isoprene concentrations. It is recommended to refine this setting by introducing a continuous or extended scaling below the lower threshold, so that the relative uncertainty increases progressively as the concentration decreases.

Response:

We have modified our uncertainty settings as suggested. Specifically, we introduce a continuous linear scaling of uncertainty for low-column grids (below 2×10^{15} molec cm⁻²), interpolated from the $2-10\times10^{15}$ molec cm⁻² range and capped at 100%. This adjustment increases uncertainties over low-column regions, improving spatial consistency with expectations. We have updated the uncertainty results throughout the manuscript, especially in Section 3.2. The uncertainty map has been updated in Fig. 2 as shown below:

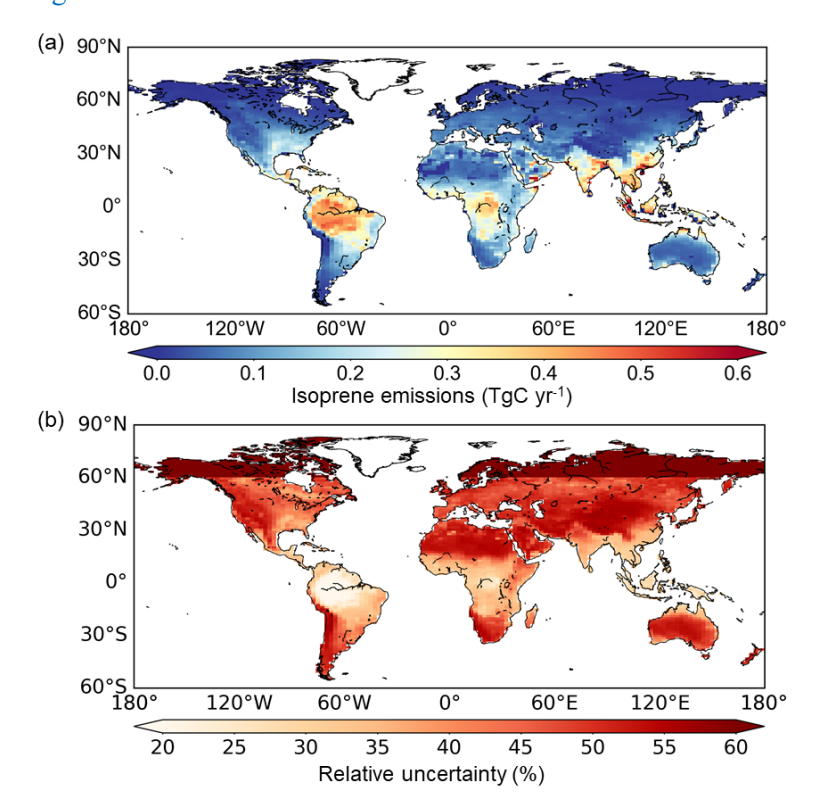


Figure 2. (a) Global distribution of isoprene emissions (TgC per grid cell of 1.27° latitude × 2.5° longitude per year) and (b) relative uncertainties (%) in 2020. The uncertainties of global totals are area-weighted averages.

Section 3.3: To validate the seasonality of the posterior emissions, comparison with inventories alone is insufficient. I suggest that the authors include HCHO-based inversion results as an additional reference.

Response:

We have added an OMI HCHO-based isoprene inversion result (Müller et al., 2024) in Figure 3 (yellow curve), which show a similar isoprene emission seasonality to our posteriors. We have added this comparison in Lines 363-366.

Lines 363-366:

"This seasonal cycle agrees with recent HCHO-based inversion results (Müller et al., 2024) but differs markedly from that in current bottom-up inventories: MEGAN-MACC (Sindelarova et al., 2014) and MEGAN-ERA5 (also known as CAMS-GLOB-BIOv3.1) (Sindelarova, 2021; Sindelarova et al., 2022) (Figs. 3 and S20)."

Table S3: The left parenthesis is missing.

Response:

We have complemented the left parenthesis.

Line 301: The use of "consistent" is not precise here, as the results are not actually identical or in full agreement in Fig. S12, please rephrase.

Response:

We have rephrased the original statement to "exhibiting a broadly similar seasonal pattern to our posteriors" in Lines 373-374.